JOURNAL OF GEOPHYSICAL RESEARCH, VOL. 114, D00K02, doi:10.1029/2008JD011575, 2009

Heavy pollution suppresses light rain in China: Observations and modeling

Yun Qian,[1] Daoyi Gong,[2] Jiwen Fan,[1] L. Ruby Leung,[1] Ralf Bennartz,[3] Deliang Chen,[4] and Weiguo Wang[1]

Received 3 December 2008; revised 6 March 2009; accepted 22 May 2009; published 15 August 2009.

[1] Long-term observational data reveal that both the frequency and amount of light rain have decreased in eastern China (EC) for 1956–2005 with high spatial coherency. This is different from the trend of total rainfall observed in EC, which decreases in northern EC and increases in southern EC. To examine the cause of the light rain trends, we analyzed the long-term variability of atmospheric water vapor and its correlation with light rain events. Results show very weak relationships between large-scale moisture transport and light rain in EC. Because of human activities, pollutant emission has increased dramatically in China for the last few decades, leading to a significant reduction in visibility between 1960 and 2000. Cloud-resolving model simulations over EC show that aerosols corresponding to polluted conditions can significantly increase the cloud droplet number concentration (CDNC) and reduce droplet sizes compared to pristine conditions. This can lead to a significant decline in raindrop concentration and delay raindrop formation because smaller cloud droplets are less efficient in the collision and coalescence processes. Together with weaker convection, the precipitation frequency and amount are significantly reduced in the polluted case in EC. Satellite data also reveal higher CDNC and smaller droplet size over polluted land in EC relative to pristine regions, which is consistent with the model results. Observational evidences and simulations results suggest that the significantly increased aerosol concentrations produced by air pollution are at least partly responsible for the decreased light rain events observed in China over the past 50 years.

Citation: Qian, Y., D. Gong, J. Fan, L. R. Leung, R. Bennartz, D. Chen, and W. Wang (2009), Heavy pollution suppresses light rain in China: Observations and modeling, *J. Geophys. Res.*, *114*, D00K02, doi:10.1029/2008JD011575.

1. Introduction

[2] Precipitation is a key physical process that links many aspects of climate, weather, and the hydrological cycle. Changes in precipitation regimes and characteristics are of great importance to humans and the entire ecosystem. One factor that could contribute to precipitation change is aerosol particles from various natural and anthropogenic sources such as urban air pollution and biomass burning. Aerosol may affect precipitation through multiple processes. The direct radiative effects of aerosols mostly act to suppress precipitation because (1) aerosols decrease the amount of solar radiation reaching the Earth surface to reduce the heat available for evaporating water and energizing convective rain clouds and (2) carboneous aerosols absorb solar radiation in the atmosphere and heat the air above the surface, which combined with less solar radiation reaching the surface, leads to stabilization of the lower atmosphere and suppression of convective clouds [e.g., *Ramanathan et al.*, 2001; *Koren et al.*, 2008; *Rosenfeld et al.*, 2008].

[3] Besides direct radiative effects, aerosols also have important microphysical effects on clouds and precipitation through their influence on cloud drop nucleation, which affects cloud life time, cloud albedo, and precipitation [*Ramaswamy*, 2001]. Observations show that aerosols generally tend to decrease precipitation for shallow or warm clouds [*Radke*, 1989; *Rosenfeld*, 1999, 2000, 2006; *Rosenfeld et al.*, 2001, 2008; *Andreae*, 2004; *Ackerman et al.*, 2003]. In other cases, however, aerosols may enhance rainfall by invigorating convection and accelerating the conversion of cloud water to precipitation [*Williams et al.*, 2002; *Koren*, 2005; *Lin et al.*, 2006; *Bell et al.*, 2008]. By combining aerosols radiative and microphysical effects in the same metric, *Rosenfeld et al.* [2008] showed a relation between aerosol optical depth (AOD), CCN concentration, and convective clouds. They found that when the AOD or aerosol concentration increases beyond a certain threshold, adding

[1]Atmospheric Science and Global Change Division, Pacific Northwest National Laboratory, Richland, Washington, USA.
[2]State Key Laboratory of Earth Surface Processes and Resource Ecology, Beijing Normal University, Beijing, China.
[3]Department of Atmospheric and Oceanic Sciences, University of Wisconsin, Madison, Wisconsin, USA.
[4]Department of Earth Sciences, University of Gothenburg, Gothenburg, Sweden.

0148-0227/09/2008JD011575$09.00

aerosols would decrease the vigor of convective clouds because both microphysical and radiative effects work in the same direction reducing the release of convective energy aloft and also reducing radiative heating at the surface. However, these conclusions were obtained under idealized cloud scale with assumption of identical meteorological forcing. As reported by *Levin and Cotton* [2007], it is difficult to establish clear causal relationships between aerosols and precipitation and to determine the sign of precipitation change in a climatological sense because changes in the ambient meteorological conditions can also influence precipitation.

[4] Asia, especially China, has been the most populated and rapidly developing region in the world during the last few decades. The ever-growing population and human activities have led to a rapid and continued increase in emission of aerosols and their precursors. For example, the number of vehicles in Beijing increased by a factor of 4, from 0.5 million in 1990 to 2 millions in 2002 [*Tang*, 2004]. With a 2.5-fold population increase emissions of fossil fuel sulfur have increased by about a factor of 9 since the 1950s [*Qian et al.*, 2006, 2007a]. These changes make China a unique region to investigate the impact of aerosols on regional climate and hydrological cycle [*Li et al.*, 2007].

[5] Many analyses based on long-term meteorological data have been performed in recent years to investigate the characteristics of decadal climate change in China. Studies have shown that much of China, particularly northern China, has undergone a warming trend caused mostly by increases in daily minimum temperature [*Wang and Gong*, 2000; *Wang and Gaffen*, 2001]. However, other regions, most notably Sichuan Basin and some areas in central and eastern China, have experienced a decrease of daily maximum temperature leading to significant cooling trends [*Qian et al.*, 1996; *Qian and Giorgi*, 2000]. On the basis of comprehensive analysis of measured pollutants and conventional meteorological records in the second half of the 20th century, it has been suggested that increased atmospheric pollutants from human activities during the past 5 decades may have produced a fog-like haze that resulted in less sunshine and solar radiation reaching the surface, reduced evaporation, moderated the warming trend, and even reduced the daytime temperature over heavily polluted areas [*Qian and Giorgi*, 1999, 2000; *Xu*, 2001; *Kaiser and Qian*, 2002; *Qian et al.*, 2001, 2003, 2006, 2007a]. Most notably, these changes have emerged despite a concurrent decreasing trend in cloud cover over China [*Qian et al.*, 2006].

[6] While many studies conducted during the past 2 decades have revealed changes in the characteristics of precipitation at various time scales over China [*Zhai et al.*, 1999; *Endo et al.*, 2005; *Ho et al.*, 2005; *Zhai et al.*, 2005; *Qian et al.*, 2007b; *Fu et al.*, 2008; *Gong et al.*, 2004], it remains challenging to identify the causes of this variability. It is believed that the long-term trend and variability of precipitation in China, which is strongly related to the Asian Monsoon, are influenced by both natural climate variability (e.g., ENSO) and anthropogenic factors (e.g., greenhouse gases, aerosols, land use change), and their interactions [*Gong and Wang*, 2000; *Gong and Ho*, 2002; *Hu et al.*, 2003; *Gao et al.*, 2003; *Menon et al.*, 2002; *Lau et al.*, 2006; *Zhao et al.*, 2006; *Gong et al.*, 2007; *Qian et al.*, 2007b]. In the past 5 decades, total precipitation has increased in southern China, especially over the middle and lower valleys of the Yangtze (Chang-Jiang) River, with more frequent and stronger flooding reported since 1990 [*Ren et al.*, 2000; *Xu*, 2001; *Gong and Ho*, 2002; *Liu et al.*, 2005]. However, drought is becoming more severe over some areas in northern China, which is consistent with decreased total precipitation and/or rain days. The water shortage in northern China is further aggravated by the growing water demand due to rapid industrial and agricultural development and population growth.

[7] Several sensitivity studies, with or without accounting for aerosol indirect effects (i.e., aerosol influence on cloud droplet size and precipitation efficiency), have been conducted to investigate the effects of aerosols on precipitation in China [e.g., *Giorgi et al.*, 2002, 2003; *Qian et al.*, 2003; *Menon et al.*, 2002; *Cheng et al.*, 2005; *Huang et al.*, 2007]. However, no consensus has yet emerged from these studies using global- or regional-scale models. While aerosol direct effects were included in these studies, the microphysical effects of aerosols on clouds and convection were typically ignored or crudely represented. There are also several studies that attempted to detect the aerosol-induced precipitation signals in observational data. *Zhao et al.* [2006] examined meteorological data and MODIS aerosol data and suggested a possible positive feedback between reduced precipitation and increased aerosol concentration over eastern central China. *Rosenfeld et al.* [2007] examined meteorological data at Mt. Hua near Xi'an, China, and found an inverse relationship between air pollution and orographic precipitation. On the basis of air pollution and various meteorological data, *Choi et al.* [2008] recently examined the impact of aerosol on precipitation frequency and *Gong et al.* [2007] found a weekly cycle of aerosol-meteorology interaction over eastern China. These studies, based on various observational data, have all revealed the potential role of aerosols on precipitation changes in China. However, owing to difficulties in isolating the influence of aerosols and meteorological conditions in the observational data, it remains a challenge to attribute changes in precipitation to air pollution, as variability and changes in the large-scale environments cannot be ignored.

[8] The goal of this study is to further elucidate the role of aerosol on precipitation in China through a combination of data analysis and modeling. In section 2 we analyze daily precipitation data from 1956 to 2005 over stations in EC to examine the long-term trend and variability of precipitation characteristics, especially light rain events. In section 3 we investigate the trends for some dominant large-scale factors, including precipitable water (PW) and water vapor transport (WVT) that could potentially affect precipitation. In section 4 we analyze the long-term trends of visual range and emissions of aerosols and their precursors, and compare their spatial patterns with that of AOD, PM_{10} concentration, cloud droplet number concentration (CDNC) and cloud droplet effective radius. In section 5 we present modeling results of three sensitivity experiments under relatively clean, moderately, and heavily polluted conditions, respectively, based on a cloud-resolving model with explicit bin microphysics. Conclusions and discussions are presented in section 6. This study is geographically focused on the eastern part of China

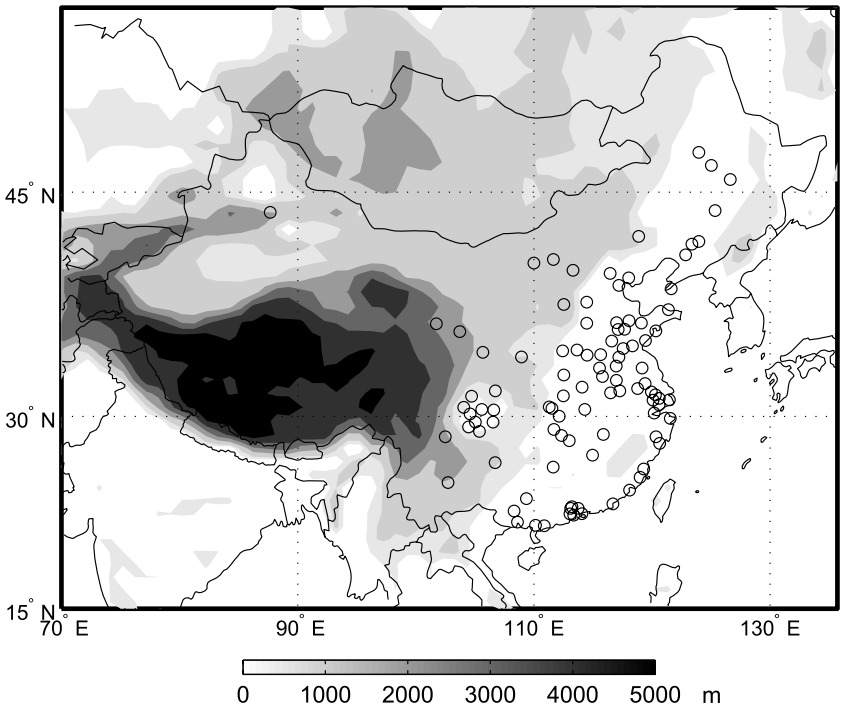

Figure 1. China's topography in shade (m) and major cities (dots) with population more than 1 million.

(see Figure 1) because of this area's (1) intense and heavy pollution, (2) dense meteorological stations and records, and (3) more frequent rain events.

2. Trends of Light Rain From 1956 to 2005

2.1. Data and Method

[9] Daily precipitation data for 194 primary meteorological stations are obtained from the China Meteorological Administration (CMA) [*Riches et al.*, 2000]. Among them, 171 stations are located in EC (east of 95°E). We screened all daily precipitation records in June-July-August (JJA) over 171 stations. A summer (JJA) with more than two missing days is regarded as a bad JJA. A station with more than two bad JJA during 1956–2005 is regarded as a bad station and excluded in the analysis. During the analysis period of 1956–2005, 147 stations have no missing data for all 50 summers, 10 stations have 1 missing day, and 5 stations have 2 missing days. The values for missing data are filled by their climatic mean of 1956–2005.

[10] In this study, a rainy day is defined as a day with either precipitation unmeasured by rain gauge (i.e., drizzle) or measurable precipitation. According to the definition of CMA, light rain days are identified as those with daily precipitation less than 10 mm (abbreviated as $p < 10$), including drizzle events. In this study we also analyzed the light rain events for those days with precipitation less than 2 mm ($p < 2$) and 5 mm ($p < 5$). We divided the EC into two subregions, north EC (NEC, north of 34°N) and south EC (SEC, south of 34°N).

2.2. Trend of Total Precipitation for 1956–2005

[11] Influenced by the abundant moisture from the southerly and southwesterly flows associated with the East Asian and Indian summer monsoon, precipitation is largest over southern China and decreases gradually from the southeastern coast to the northwestern inland in China [*Qian and Leung*, 2007]. The annual total rainfall is over 1500 mm in Southeast Coast, Pearl River, and the lower Yangtze River Basin, but less than 100 mm in the northwestern region.

[12] Figures 2a and 2b show the spatial pattern of trends for summer and annual precipitation amount, respectively, estimated using least squares technique. From 1956 to 2005, much of the southern part of EC has exhibited an increase in total precipitation in summer. The maximum increase of total precipitation is over the lower Yangtze River basin, with an increase of 1–5% per decade. Much of the northern part of EC, more specifically along the Yellow River and Hai River basins, has exhibited a statistically significant decrease in total precipitation. The decreasing trend reaches 2–10% per decade. The annual mean precipitation exhibits a similar trend compared to summer precipitation because summer is the major rainy season in EC. This pattern of precipitation variation has been documented as "South Wet and North Drought" [*Gong and Ho*, 2002; *Hu et al.*, 2003].

[13] Figures 2c and 2d show the time series of summer and annual precipitation anomaly (in percentage) averaged over SEC, NEC, and the whole EC, respectively, for 1956–2005. While the trend of mean precipitation averaged over all stations in EC shown in Figures 2a and 2b is very small, the summer precipitation amount increased 2.3% per decade in SEC and decreased 2.1% per decade NEC, respectively, and both are statistically significant at the 95% significance level. The annual mean precipitation also exhibits a similar trend averaged over SEC, NEC, and EC but with a smaller magnitude compared to summer precipitation.

2.3. Trend of Light Rain for 1956–2005

[14] Although the amount of precipitation contributed by light rain accounts for only 25% of total precipitation in the

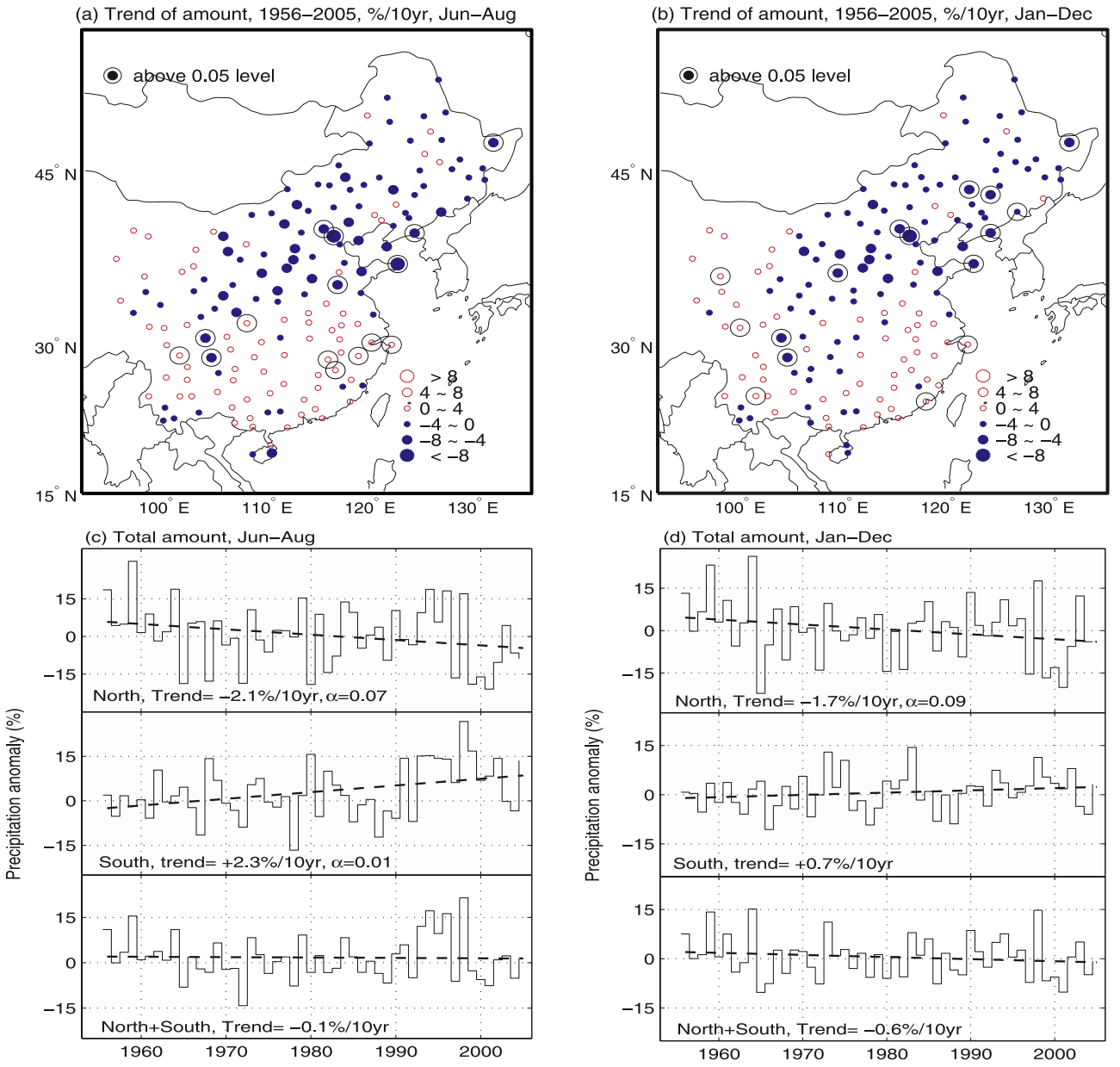

Figure 2. Spatial distribution of trends (% per decade) from 1956 to 2005 for (a) June–July–August (JJA) and (b) annual precipitation amount and time series of (c) JJA and (d) annual precipitation anomaly (%) from 1956 to 2005 averaged over northern East China (top), southern East China (middle), and whole East China (bottom). Station trend indicators with circle around them are significant at the 95% confidence level.

NEC and 17% in the SEC, respectively, the number of light rain days ($p < 10$) accounts for around 83% in the SEC and 74% in the NEC in total number of rainy days during summer. Therefore, the majority of precipitation events are light rain in EC.

[15] Figures 3a and 3c show the spatial distribution of linear trends of number of summer light rain days with $p < 2$ mm $d^{-1}$and $p < 5$ mm d^{-1}, respectively, estimated using least squares technique. While total precipitation exhibits a trend of "South Wet and North Drought," both the number of rainy days and precipitation amount from light rain events (not shown) present a spatially consistent decreasing trend over the entire EC, regardless of the thresholds (2 mm versus 5 mm d^{-1}) used to define light rain. Out of the 162 stations, 159 show decreasing trends for light rain less than 2 mm d^{-1}, and 156 show decreasing trends for light rain less than 5 mm d^{-1}. The number of light rain days has declined by 1–4 days per decade. The trends are statistically significant at 95% significance level over the majority of stations (121 out of 162 for $p < 2$ and 118 out of 162 for $p < 5$, respectively). Only a very few stations, which are randomly located, show positive trends but none of them are statistically significant at 95% significance level. Figures 3b and 3d show the spatial distribution of linear trends of annual total number of light rain days. All stations exhibit decreasing trends by 5–20 days per decade

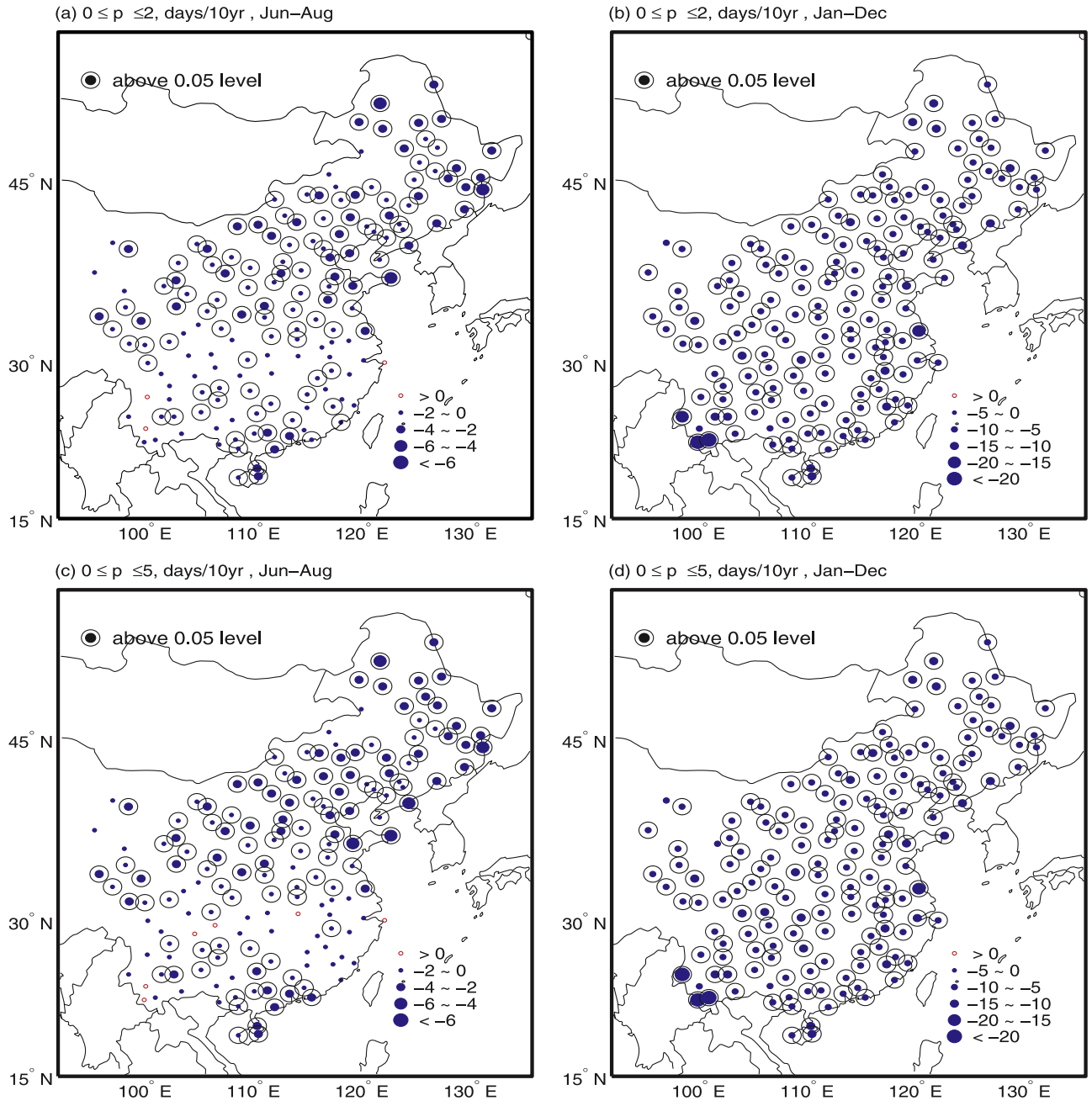

Figure 3. Spatial distribution of trends (days per decade) from 1956 to 2005 for JJA light rain events (a) less than 2 mm d^{-1} and (c) less than 5 mm d^{-1} and annual light rain events (b) less than 2 mm d^{-1} and (d) less than 5 mm d^{-1}. Station trend indicators with circle around them are significant at the 95% confidence level.

for light rain events for both $p < 2$ mm d^{-1} and $p < 5$ mm d^{-1} and the trends are statistically significant at 95% significant level over majority of stations.

[16] Figure 4a shows the time series of number of days with light rain ($p < 10$) averaged over SEC, NEC, and EC, respectively, for summer of 1956–2005. All three panels show decreasing trends. The light rain days decreased 2.3 days per decade in NEC and decreased 1.2 days per decade in SEC, both are significant at the 99% significance level. Averaged over EC, the decreasing trend of light rain days is −1.8 days per decade. In association with the declined rainy days, JJA precipitation amount contributed by light rains has decreased by 2.8% per decade for NEC and 1.1% per decade for SEC, respectively. Similarly, as shown in Figure 4b, annual light rain days decreased 6.9, 8.1 and 7.4 days per decade in NEC, SEC and EC, respectively. The annual precipitation amount contributed by light rains has decreased by 2.0% per decade for NEC and 1.3% per decade for SEC.

[17] To take a broader look at the changes in precipitation characteristics, we examined the trends of rainy days and rainfall amount as a function of precipitation rates [*Fu et al.*,

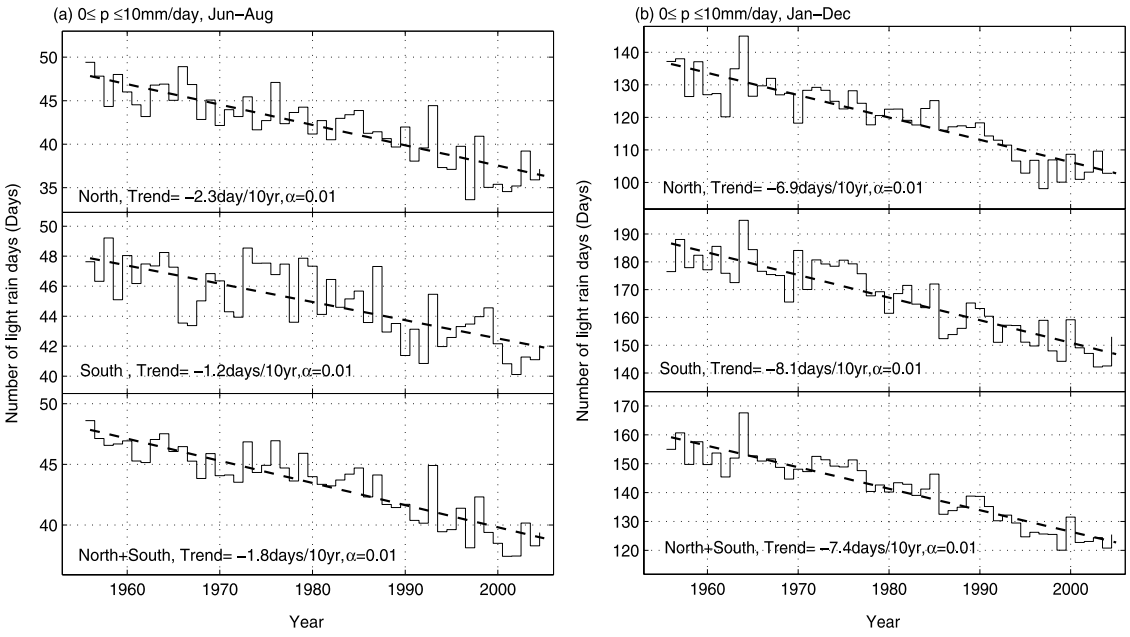

Figure 4. The time series of number of days for light rain (less than 10 mm d^{-1}) from 1956 to 2005 for (a) JJA and (b) annual precipitation over northern East China, southern East China, and entire East China (days).

2008]. Figure 5 displays the trends from 1956 to 2005 for rainy day frequency and rainfall amount at 10 precipitation bins averaged over EC. Decreasing trends for both rainy days and rainfall amount are apparent for light rain with precipitation rate less than 10 mm d^{-1}. The most significant changes are found for lighter rain with daily precipitation less than 2 mm d^{-1}, mainly contributed by drizzle. Furthermore, rainy days decreased by more than 5.2% (6.3%) per decade and rainfall amount decreased by 2.7% (2.9%) per decade for light rain less than 2 mm d^{-1} in the summer (all 12) months. For rain events with precipitation rate larger than 10 mm d^{-1}, both positive and negative trends can be found, but not statistically significant at 95% level. For extreme event with daily precipitation larger than 50 mm d^{-1}, a remarkable increase trend for both precipitation amount and rainy days can be found, implying that heavy precipitation has become more severe and more frequent. Together with the significant light rain reduction, this evidence suggests a shift of precipitation rate from light to heavy rain. Since the majority of precipitation events are light rain in EC, the frequency of precipitation (in all rates) shows a decrease trend in both SEC and NEC (not shown) in both summer and annual mean.

3. Trends of Large-Scale Atmospheric Fields

3.1. Data

[18] Atmospheric circulation data used in this section are from the European Centre for Medium-Range Weather Forecast (ECMWF) 40-year reanalysis (ERA40) [*Uppala et al.*, 2005], which includes geopotential heights, temperature, wind vector, and humidity from 1000 hPa to 100 hPa levels. ERA40 covers a time period from September 1957 to August 2002 and is archived on a 2.5° × 2.5° longitude-latitude grid. Monthly mean are obtained by averaging daily data.

3.2. Precipitable Water

[19] A large-scale factor that correlates well with precipitation is the column total water vapor, or precipitable water (PW), in the atmosphere [*Zhai and Eskridge*, 1997; *Simmonds et al.*, 1999; *Zhou and Yu*, 2005]. PW is defined as

$$PW = \frac{1}{g}\int_{100hPa}^{1000hPa} qdp \tag{1}$$

where g is the acceleration of gravity and q is the specific humidity. Figure 6 shows the JJA mean PW trends from 1958 to 2002 on the basis of the ERA40 data. A slight but not statistically significant increase trend can be seen over the majority of EC, except for a small area near Bo-Hai bay. Regional mean trend of PW over the entire EC (20−45°N, 100−122.5°E) is 0.27 kg m^{-2} $decade^{-1}$ (0.57%/10 years) which is statistically significant at the 90% confidence level. The increase trend is even stronger in the later 2 decades, and regional mean PW shows a trend of 0.65 kg m^{-2} $decade^{-1}$ (1.4%/10 years) at the 90% confidence level. While the trends are not evident in the NEC, PW shows an increase trend at the 90% confidence level over the SEC (30°N and 30°S), and the magnitude of trend increases from 1% to 6% per decade from SEC coast to South China Sea. Annual mean PW exhibits a very similar trend compared to summer PW.

[20] If the trends in light rain are related to changes in large-scale moisture content in the atmosphere, we may expect a decreasing trend in PW generally over China. Instead, Figure 6 shows an increasing trend in PW, partic-

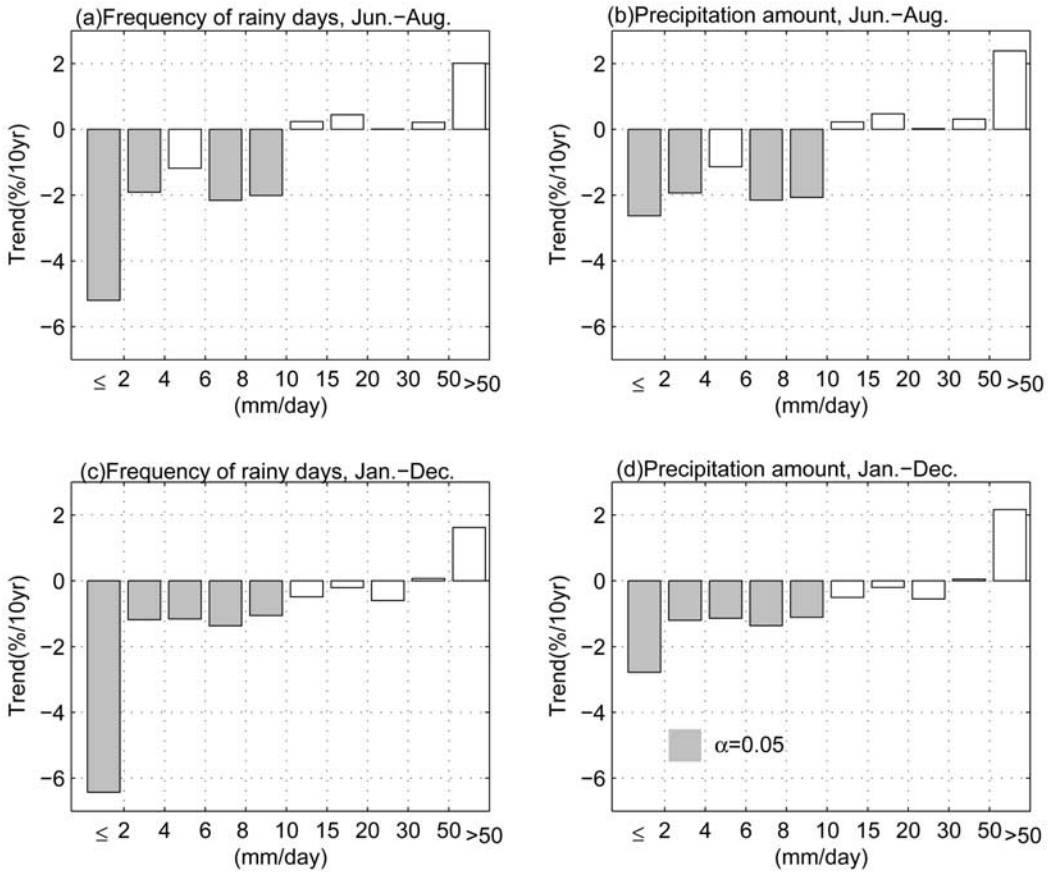

Figure 5. Linear trends of frequency of (a) JJA and (c) annual rainy days and of (b) JJA and (d) annual precipitation amount as function of precipitation bins, averaged over East China (EC) from 1956 to 2005 (% per decade).

ularly in SEC, that contradicts the significant decrease in the light rain events in EC.

3.3. Regression Analysis for Water Vapor Transport and Light Rain

[21] To further investigate possible influence of large-scale circulation changes such as water vapor transport (WVT) on the light rain trends in EC, we performed a regression analysis between light rain in EC and the vertically integrated moisture transport (Q). Here Q is defined as

$$Q = \frac{1}{g}\int_{500hPa}^{1000hPa} q \bullet V dp \qquad (2)$$

where V is the horizontal wind vector and q is the specific humidity. Moisture transport above 500 hPa is neglected as its contribution to the total column moisture transport is relatively small. Q is decomposed into water vapor transport in the zonal (Qu) and meridional (Qv) components. Light rain frequency in EC, x, is calculated by averaging the light rain frequency for each summer (i.e., the fraction of the total number of days with light rain during the 92 days in JJA) over all stations in EC, and normalizing the frequency by the long-term averaged frequency between 1958 and 2002. We then calculated the regression coefficients (bu and bv)

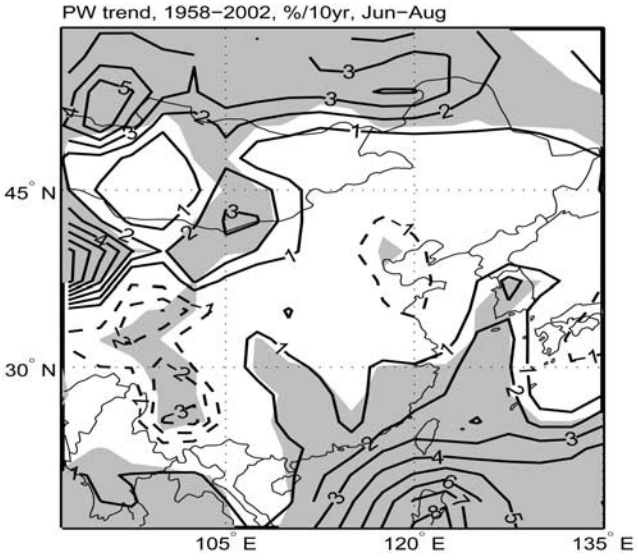

Figure 6. Spatial distribution for trend of column total precipitable water (PW) in JJA from 1958 to 2002 based on ERA40 data (% per decade). Areas are shaded at the 95% significance level.

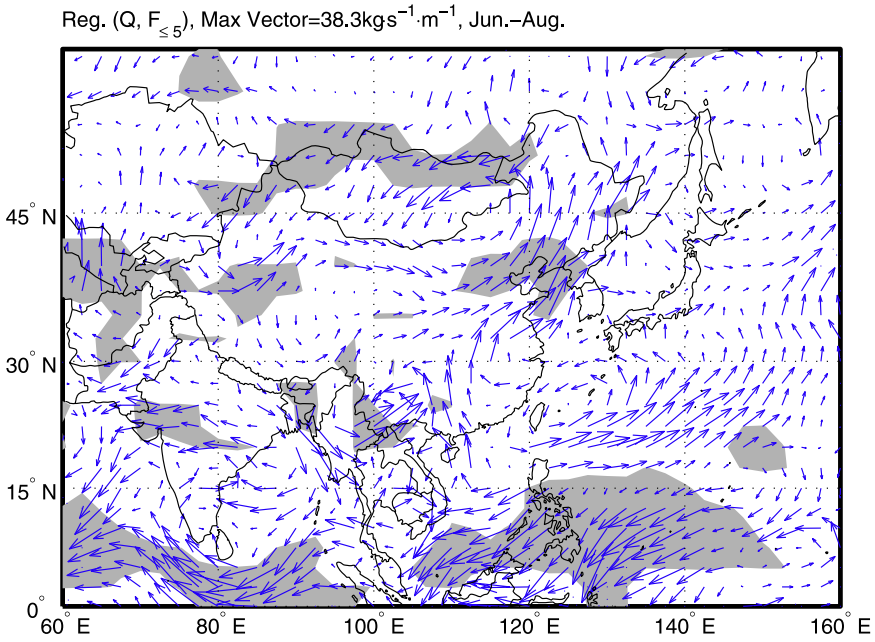

Figure 7. Regression of vertical integrated (1000–500 hPa) water vapor transport (WVT) to number of light rain (<5 mm d^{-1}) days for JJA of 1958–2002 over East Asia. Areas are shaded at the 95% significance level.

between Qu and x, and Qv and x, respectively, based on the following:

$$bu = ru^* \frac{\sigma(Qu)}{\sigma(x)} \tag{3}$$

$$bv = rv^* \frac{\sigma(Qv)}{\sigma(x)} \tag{4}$$

where ru (rv) is the correlation coefficient between Qu (Qv) and x, and $\sigma(Qu)$, $\sigma(Qv)$ and $\sigma(x)$ are the standard deviation of Qu, Qv, and x, respectively [*Wilks*, 1995].

[22] As discussed in section 2.2, summer precipitation in China is strongly influenced by the prevailing southerly and southwesterly moisture transport associated with the monsoonal flows. Figure 7 shows the regression of vertically integrated moisture transport with light rain frequency ($p <$ 5 mm d^{-1}) for all the summers between 1958 and 2002. The values of bu and bv are shown using arrows to represent both the magnitude and direction of moisture transport that favors light rain in EC. Shaded areas indicate that ru and rv are significant at the 95% confidence level.

[23] While the summer precipitation amount is well correlated with the vertically integrated moisture transport (not shown), Figure 7 shows that there is no spatially coherent moisture transport pattern that favors light rain frequency in EC. Although there are isolated regions in Bo-Hai Bay, North Indian Ocean, and South China Sea where the regression exceeds the statistically significant level, the moisture transport connecting those regions to EC is not apparent. This indicates that the correlation between light rain events in EC and large-scale moisture transport is weak during 1958–2002. The same conclusion can be drawn on the basis of light rain events defined using the 2 and 10 mm d^{-1} thresholds (not shown).

[24] On the basis of the analysis of PW and WVT, we found no supporting evidence that the decreasing light rain trend in EC during the past 5 decades may be related to changes in the large-scale moisture content and its transport. Indeed, we are not aware of any working hypothesis by which the large-scale atmospheric conditions can lead to opposite trends in total precipitation and light rain as observed in EC. This strongly suggests that other mechanisms may play a dominant role in altering the precipitation characteristics in EC.

4. Variation of Air Pollution, Aerosols, and Cloud Droplets in China

[25] Air pollution and aerosol data used here include sulfur emission, PM_{10}, visual range and AOD. Sulfur emission data are from *Ren et al.* [1997] and *Giorgi et al.* [2002]. Visual range in China was recorded by several bins of range before 1980 and by real distance after 1980 (see Figure 9) [*Qian and Giorgi*, 2000]. Visual range data are corrected on the basis of relative humidity so days with fog are eliminated in the study [*Rosenfeld et al.*, 2007]. PM_{10} is measured in major cities of China using the ambient air pollution index (API). The daily API and the corresponding pollutants (PM10, SO_2, or NO_x) have been archived at the State Center of Environment Monitoring of China [see *Gong et al.*, 2007]. We also used MODIS AOD data from *Levy et al.* [2007] and *Remer et al.* [2008] in this analysis.

[26] Figure 8 shows the spatial distribution of PM10, corrected visual range, AOD and sulfur emission over EC. Air pollution is most prominent over the eastern part of China, which accounts for more than 80% of population and GDP. Maximum values are located over Sichuan Basin,

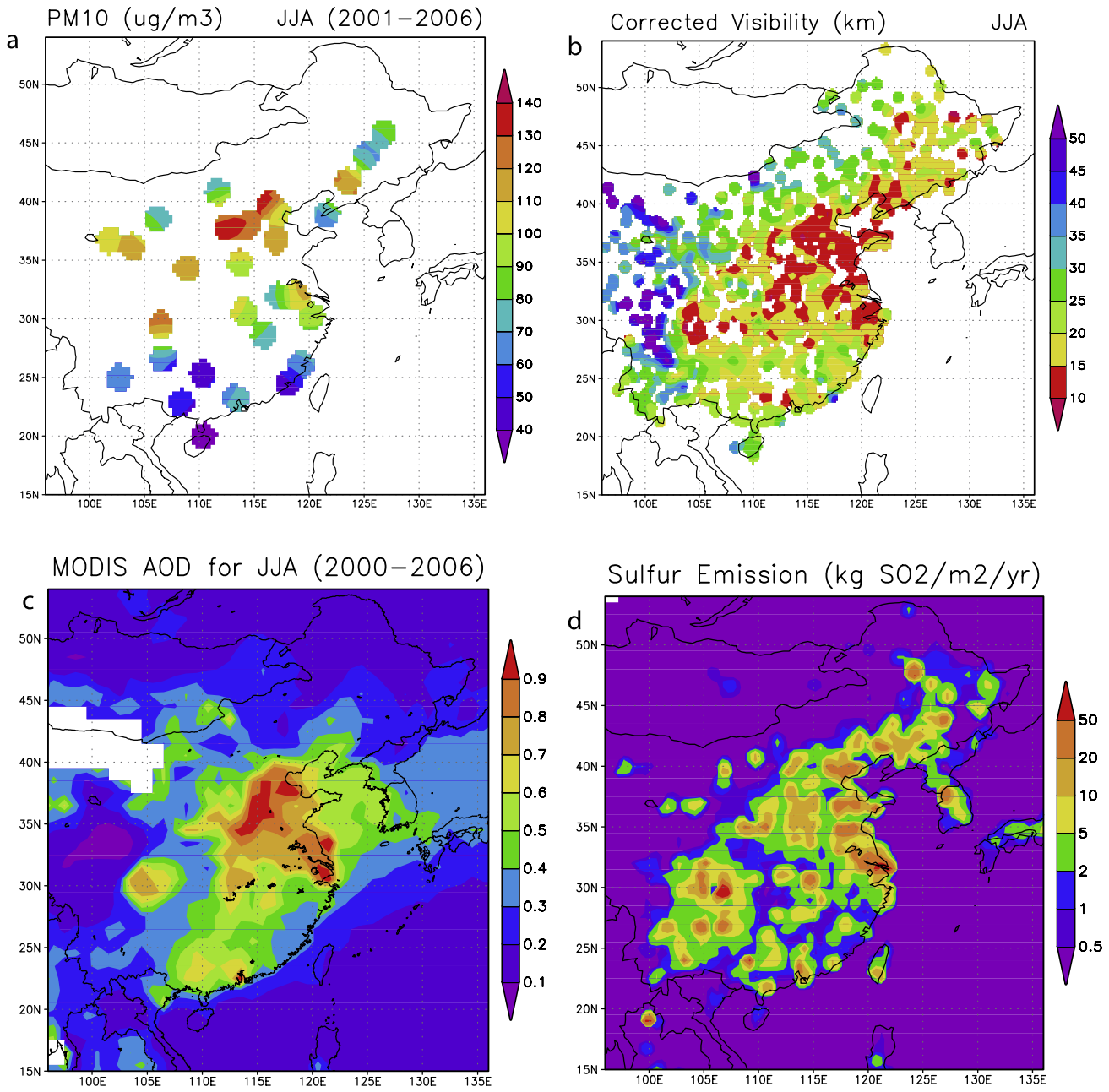

Figure 8. (a) Observed JJA mean PM10 concentration (μg m^{-3}), (b) corrected visual range (km), (c) MODIS aerosol optical depth, and (d) sulfur emissions (kg SO_2 m^{-2} a^{-1}) over East China.

Hua-Bei plain (including Shanxi and Shandong provinces), the Beijing-Tianjin megacity clusters, and Yangtze delta megacity clusters, both clusters are among the fastest developing regions in China. Observed PM10 concentration, visual range and AOD exhibit a consistent spatial pattern. They are also very well spatially correlated with the pollutants (e.g., sulfur) emissions from human activities, which imply that anthropogenic emission is the major source of air pollution and atmospheric aerosols in China.

[27] We are not able to calculate the long-term trend for PM_{10} and AOD because data are not available for the earlier period of 1950s–2000s. However, we have more than 40 years of data for sulfur emission and visual range. Figure 9 shows that the total emissions of SO_2 in China had continuously increased from 1954 to 2000, with a few peaks around the early 1960s, early 1980s, and later 1990s, respectively. We don't have the measured emission data for other aerosols, such as Black Carbon (BC) or Organic Carbon (OC), for the complete 40 years, partly because the sources for those aerosols are more diverse. But it is no doubt that BC and OC aerosols have been increasing in the past 5 decades because (1) BC and OC share some common sources of emission with sulfur (e.g., fossil fuel burning) and (2) population and intensities of human activities have been increasing, although the increase rate may differ from that of sulfate. It can be seen from Figure 9 that the visual range has dropped dramatically in China from 1960 to 2000 while pollutant emission has gone up significantly. The

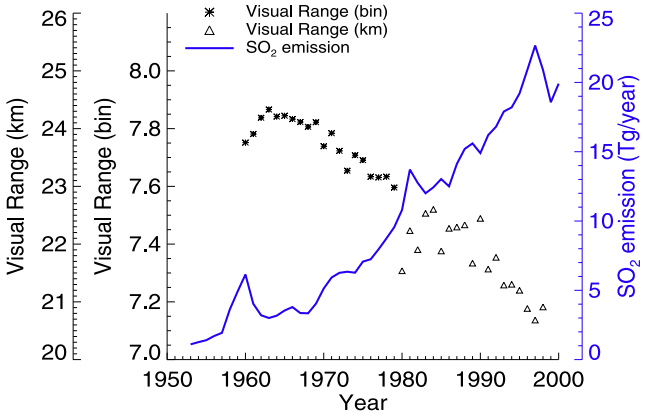

Figure 9. Time series of China total SO_2 emission (Tg a^{-1}) for 1953–2000 and corrected visual range (bin before 1980 and km after 1980) over East China for 1960–2000.

consistent spatial pattern and temporal trends between the pollutant emission and visual range suggest that the increased atmospheric pollutant resulting from human activities may have produced a haze that significantly reduced the visual ranges in the past 5 decades in China. But what was the effect of aerosols on cloud properties and precipitation?

[28] Since cloud droplets form on preexisting aerosol particles that act as cloud condensation nuclei (CCN), increased concentrations of atmospheric aerosol particles not only affect visual range but also change the size distribution of cloud droplets, thus affecting clouds properties, as well as precipitation characteristics (e.g., timing and rain rate distribution). Figure 10 shows the spatial distribution of cloud droplet number concentration (CDNC) and cloud effective radius for water clouds (CERW) averaged for 2003–2006. CDNC and CERW used in this study are derived from Moderate Resolution Imaging Spectroradiometer (MODIS) data using the methodology described by *Bennartz* [2007]. This study utilizes the level-3 daily atmospheric product, termed Atmospheric Daily Global Joint Product (collection 5) available at NASA Goddard Earth Sciences (GES) Distributed Active Archive Center (DAAC). The data are available on a 1 × 1 degree grid. A subset of the daytime cloud parameters, which includes cloud fraction, cloud top temperature, effective radius, liquid water path, and optical depth was extracted and used in this study (see *Platnick et al.* [2003] and *King et al.* [2003] for details). Using cloud top temperature thresholds and cloud flag information, the MODIS data are screened to exclude any possible contamination with ice clouds. Furthermore, a minimum cloud cover of 50% within each 1 × 1 degree grid was required to ensure reasonable statistics and retrieval accuracy. A detailed description of the data screening and derivation of CDNC is given by *Bennartz* [2007]. It should be noted that the original work by *Bennartz* [2007] was only applied to marine stratus clouds. While the technique in principle also works for clouds over land, the variable surface albedo may introduce additional uncertainties. Furthermore, the presence of high aerosol loads in the clouds or in the free atmosphere above the clouds may also have an impact on the CERW and CDNC retrievals (see *Bennartz and Harshvardhan* [2007] for a discussion of the impact of aerosol on cloud microphysical retrievals). Therefore, the resulting images of CDNC and CERW need to be interpreted with caution, especially with regard to the absolute values of CERW and CDNC.

[29] It can be seen from Figure 10a that CDNC is significantly higher over EC than the adjacent land (e.g., India and Southeast Asia) and ocean areas. CDNC reaches 200 per cm^3 over EC and the ocean downwind, but the highest concentrations are located over Sichuan Basin and central EC. CDNC is usually below 120 per cm^3 over more remote oceanic air. The spatial distribution of CDNC is very well correlated with that of PM10, AOD, visual range and pollutants emission shown in Figure 8, which indicates that higher aerosol and CCN concentrations contribute to higher CDNC.

[30] Under otherwise identical conditions an increase in the number of available CCN will result in an increase in CDNC. It will also simultaneously result in a decrease in CERW, since liquid water will be distributed over more droplets. Figure 10b shows that CERW, with larger size droplets over pristine ocean and smaller ones over polluted land and downwind ocean, is spatially anticorrelated with CDNC. The mean CERW is around 14–20 μm over pristine ocean and 8–12 μm over polluted areas. As pointed out by *Brenguier et al.* [2000] CERW will additionally be affected by the variations in cloud geometrical thickness within an

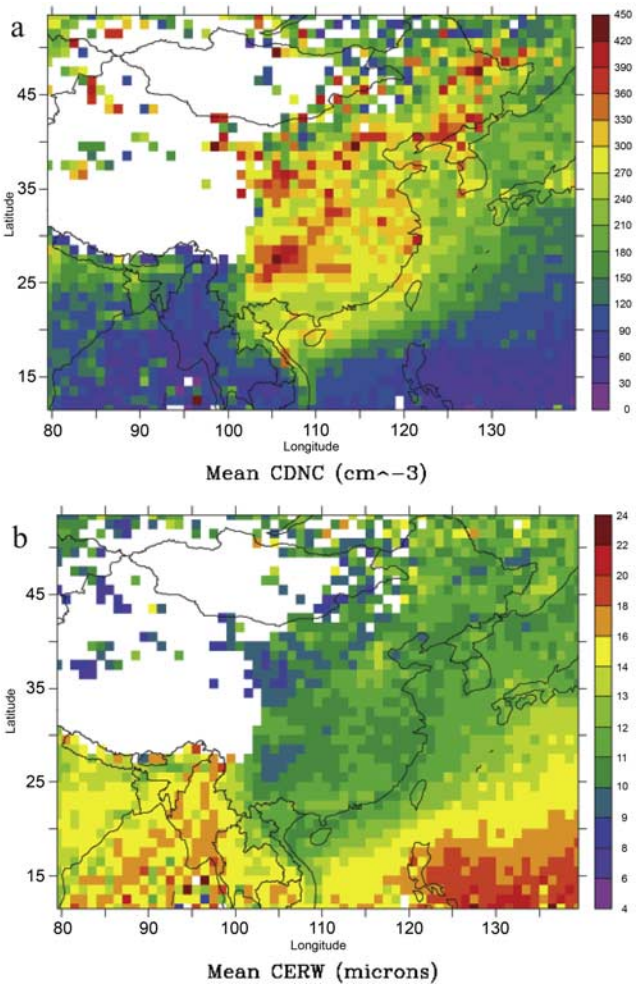

Figure 10. The spatial distribution for cloud droplet number concentration (CDNC, cm^3) and cloud effective radius for water clouds (CERW, μm) averaged for 2003–2006.

observed cloud field, because the cloud top effective radius increases with increasing cloud geometrical thickness. Thus, while both quantities in principle are sensitive to changes in ambient aerosol conditions, CDNC will show a clearer relation between the availability of CCN and cloud microphysical parameters than CERW.

[31] These results from satellite data in China are generally consistent with the first indirect effect of aerosol; that is, more aerosol particles lead to more cloud droplets but with smaller average drop size under identical ambient fields. Analysis of cloud drop size for several regions and weather regimes around the world suggest a drop radius of 12 μm for warm rain threshold [*Andreae*, 2004; *Rosenfeld*, 2006]. Our analysis of long-term averaged CERW suggests a higher likelihood for precipitation to be found in the pristine oceans (mean CERW of 14–20 μm) than polluted regions (mean CERW of 8–12 μm). We will further investigate how precipitation may be affected by aerosols through cloud-resolving modeling described below.

5. Cloud-Resolving Model Simulations

[32] As introduced in section 1 the observations show that aerosols generally decrease precipitation in shallow or warm clouds. Meanwhile aerosol may also stabilize the lower atmosphere and suppresses the generation of convective clouds through their radiative effects [*Fan et al.*, 2008]. Those effects may be applied, at least partly, to explain the observational evidence (i.e., decreased light rain events) presented in section 2. However, in some cases aerosols may enhance rainfall, particularly heavy rainfall, by invigorating convection [e.g., *Khain et al.*, 2005; *Fan et al.*, 2007a]. *Khain et al.* [2008] shows that the ambient meteorological conditions such as relative humidity can play a significant role in determining whether aerosols increase or decrease precipitation. To further investigate the role of aerosols on precipitation changes in China, we include a modeling component to provide further insights on how aerosols may affect light precipitation.

[33] We employ a cloud-resolving model referred as the System for Atmospheric Modeling (SAM) [*Khairoutdinov and Randall*, 2003] coupled with an explicit bin microphysics based on *Khain and Pokrovsky* [2004] to simulate aerosol effects on precipitation. SAM uses the dynamical framework of the large eddy simulation (LES) model of *Khairoutdinov and Kogan* [1999] to solve the equations of motion using the inelastic approximation. The spectral bin microphysics (SBM) solves a system of equations for eight number size distributions for water drops, ice crystals (columnar, plate-like, and dendrites), snowflakes, graupel, hail/frozen drops and aerosol particles. Each size distribution is represented by 33 mass doubling bins; that is, the mass of a particle m_k in the k bin is determined as $m_k = 2m_{k-1}$. All relevant microphysical processes/interactions including droplet nucleation, primary and secondary ice generation, condensation/evaporation of drops, deposition/sublimation of ice particles, freezing/melting, and mutual collisions between the various hydrometeors are calculated explicitly [*Khain and Pokrovsky*, 2004]. With the size-resolved aerosol and cloud microphysics, aerosol effects on clouds and precipitation can be better addressed.

[34] Details about the nucleation of droplets and ice crystals can be found in the work of *Khain and Pokrovsky* [2004] and *Fan et al.* [2009]. In this study, ice nucleation through the deposition and condensation freezing modes is calculated using the parameterization of *Meyers et al.* [1992]. Ice nucleation via immersion freezing is incorporated using the parameterizations based on the stochastic hypothesis formulated by *Bigg* [1953]. Contact freezing as a primary ice nucleation mechanism is neglected since contact freezing seems to be much less efficient when the number of immersion and contact IN are of the same order because of low collision efficiency [*Lynn et al.*, 2005]. The longwave and shortwave radiation scheme from the National Center for Atmospheric Research (NCAR) Community Atmospheric Model (CAM3.0) [*Kiehl et al.*, 1998] is employed to calculate the radiative effects of clouds.

[35] Three simulations, representing clean (C case), moderately polluted (M case), and heavily polluted conditions (P case), are performed to study aerosol effects on precipitation in EC. The total aerosol concentration (N_a) is set to be 1085, 5425, and 10850 cm^{-3}, for the C case, M case, and P case, respectively. Measurements [e.g., *Shi et al.*, 2007; *Gao et al.*, 2007; *Chan and Yao*, 2008] show that the total N_a in urban areas can reach $1.0 \times 10^4 - 8.0 \times 10^4$ cm^{-3} in China. *Gao et al.* [2007] measured a N_a number of 10670 cm^{-3} during summer in Jinan, a city in central EC. Therefore, an aerosol concentration of 10850 cm^{-3} represents a typical polluted condition in the EC region. *Qian et al.* [2006] shows that the pollutants emission resulting from fossil fuel consumption increased ninefold from 1950s to 2000s. To assess the impacts of aerosols on precipitation changes in the last 50 years, we prescribe N_a in the C case to be about one tenth of the present value.

[36] The shape of aerosol size distribution is kept to be the same in all simulations. The initial aerosol size distribution is adopted from the typical continental case of *Khain et al.* [2005]. The computational domain is composed of 720 km and 24 km in horizontal and vertical directions, respectively, with a horizontal resolution of 500 m, and the vertical coordinates are stretched with resolution varying from 100 m in the lower atmosphere to 400 m in the upper atmosphere. Periodic lateral boundary conditions are used. The dynamic time step is 2 s and radiation calculation is called every 3 min. The sounding used to initialize the model dynamical fields is derived from Shouxian, Anhui province of China (32.5°N, 116.8°E), measured during the GAME/HUBEX field campaign in 1999 [*Ding et al.*, 2001]. More details about this HUBEX data and the regional climate in this region can also be found in the work of *Leung et al.* [2004]. The observed forcing data are used to constrain the simulations every 6 h, while the observed sensible and latent heat fluxes are applied to the simulations every 4 h. Since our simulation is 2-D and only run for 1.5 days, it is not very realistic to compare the model results with the point measured or area average precipitation rates. Nevertheless, our simulation captures the storm and the stratiform and anvil clouds induced by the storm.

[37] Shouxian, approximately 500 km west of Shanghai, is also a central location in EC. During summer, there is abundant precipitation and high aerosol loadings from man-made sources. Except for the aerosol concentrations, the simulation setups are identical in all three cases. Our choice

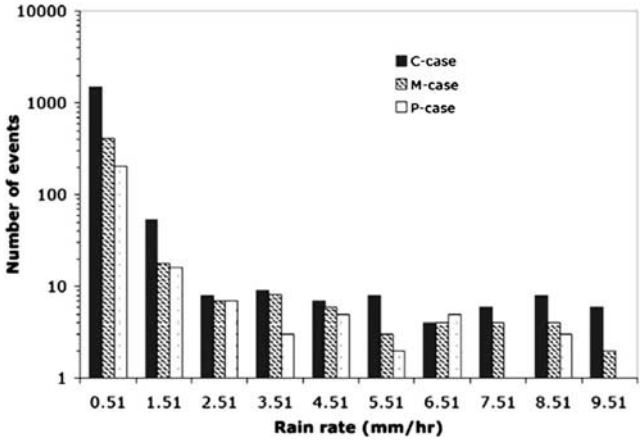

Figure 11. Sum of frequencies of rainy events (number of events) as function of rain rate for clean (C case), moderately (M case) and heavily polluted (P case) cases over the whole time period of simulations.

of simulating the meteorological conditions of Shouxian is also motivated by measurements that will become available through the U.S. Department of Energy's Atmospheric Radiation Program (ARM) mobile facility deployed at Shouxian from April to December 2008, to acquire essential cloud, aerosol, radiative, and meteorological measurements for the study of aerosol indirect effects in China.

[38] The precipitation frequencies for low and median rain rates (<10 mm h^{-1}) are presented in Figure 11 for the three experiments. Precipitation frequency of the P case is significantly lower than that of the C case in almost all lower rain rates. The maximum rain rate in the P case is 9.6 mm h^{-1}, which is about 6 times lower than that in C case. The distribution of precipitation rates for the M case is mostly between the C case and P case, but closer to the latter. The total precipitation in the low and median rain rates in the P case and M case are reduced by over 85% and 70%, respectively, relative to the C case. Although the modeled clouds do not present all cloud cases in the summer of EC, the significant reduction of precipitation frequencies in low rain rates indicates that

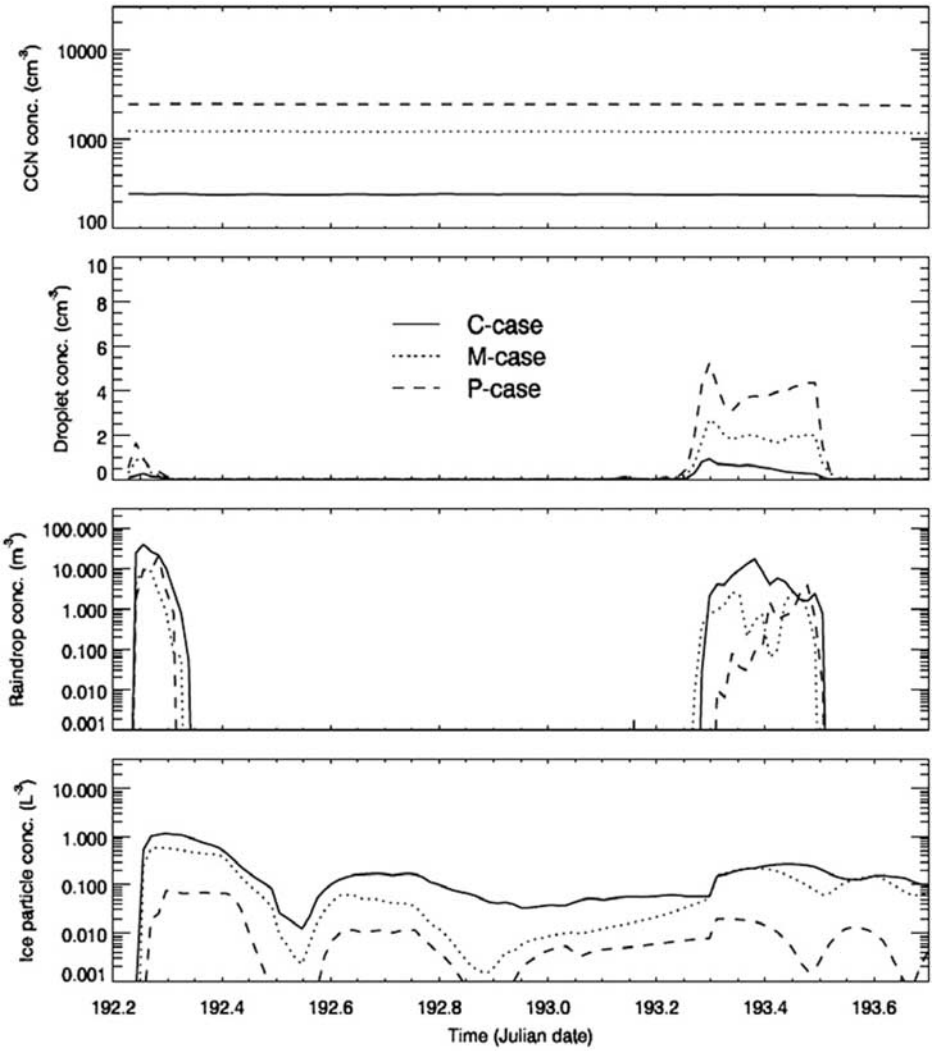

Figure 12. Time series of cloud condensation nuclei (cm^3), cloud droplet (cm^3), raindrop (m^3), and ice particle (L^3) concentrations for clean (C case), moderately (M case), and heavily polluted (P case) cases averaged over a subdomain, including the major cloud fields with the size of 450 km.

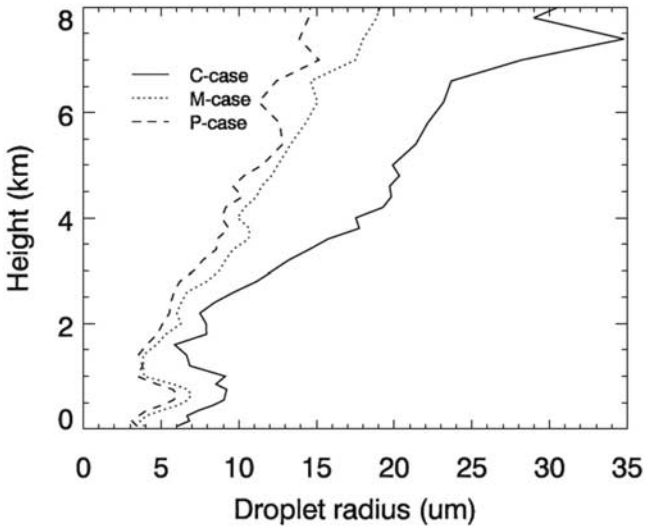

Figure 13. Vertical profiles of water drop (cloud droplet + raindrop) radius (μm) for clean (C case), moderately (M case), and heavily polluted (P case) cases.

increased aerosols potentially decrease light rain frequencies over the polluted areas.

[39] Figure 12 shows the cloud microphysical properties from the three cases to illustrate the suppression process of precipitation induced by aerosols. With the increase of aerosol concentration by 10 times from the C-to-P cases, CDNC increases by about 4–5 times, which is qualitatively consistent with satellite observations over EC and the remote oceanic area within the domain (Figure 10a). Figure 12 shows that raindrop concentration is significantly reduced and the formation of raindrop is delayed in the M case and P case, because collision and coalescence are much less efficient when droplet sizes are much smaller (see Figure 13). The water drop radius (including cloud droplet and raindrop) in the P case is reduced by up to 50% relative to C case, which is also consistent with the satellite observation for CERW (Figure 10b). Ice particle concentrations in the P case are about 10 times lower than those in the C case as shown in Figure 12. Since aerosols are not directly used as ice nuclei (IN), ice formation is only related to ice supersaturation and supercooled droplets above the homogeneous freezing level in the simulations. Therefore, the lower ice particle concentrations in the M case and P case are mainly related to the much weaker convective strength, which lowers ice production as ice supersaturation is reduced and less cloud droplets are transported to the higher levels. Indeed, the maximum updraft velocity is 28.6 m s^{-1} in the M case, and it is 19.5 m s^{-1} in the P case, which is about 2 times lower than that in the C case. The suppression in convection in the polluted cases probably results from much stronger evaporation due to much more small droplets [*Rosenfeld et al.*, 2008]. In addition, the radiative effects of clouds that result from higher hydrometeor concentration and smaller sizes could also cause stronger cooling and suppress convection. It should be noted that only aerosol indirect effect is considered in the simulations. Including aerosol direct radiative effect would lead to further suppression of convection due to the reduction of surface heat fluxes [*Fan et al.*, 2008]. The significant reduction in convection and precipitation under the moderately and heavily polluted conditions is consistent with the processes discussed by *Rosenfeld et al.* [2008]; that is, high CCN concentrations were found to suppress convection and precipitation in both observational and modeling studies [*Rosenfeld*, 2000].

[40] These model results suggest the plausibility that low and median precipitation rates can be significantly reduced when CCN concentration is increased by 5–10 times. It is noted that some properties such as droplet size and precipitation rate do not change as significantly as droplet and ice number concentrations from the M case to the P case because these quantities are limited by available total water content. This is consistent with past studies [*Fan et al.*, 2007b] that cloud droplet size and precipitation rate become much less sensitive to further increase of CCN concentrations in a polluted environment.

6. Conclusions and Discussions

[41] Precipitation is a key physical process that links many aspects of climate, weather, and the hydrological cycle. Long-term observational data reveal significant spatially coherent decreasing trends in both the frequency and amount of light rain in East China (EC) from 1956 to 2005. This feature is different from the pattern of total rainfall observed in EC, which shows a decrease trend in the northern part of EC (NEC) and an increase trend in the southern part of EC (SEC). The difference in light rain and total rainfall trends motivates this study to examine factors that may lead to a shift in rain rates that is evident in EC since the 1950s.

[42] We first examined the role of the large-scale moisture and its transport. We analyzed the variation of precipitable water (PW) and specific humidity, and found no evident trends in NEC. However, a small increase trend of PW is observed over SEC, which could provide a favorable moisture condition for precipitation. The increase of PW in SEC may partly explain the increase of precipitation amount in South China; however, it contradicts with the significant decrease trend in light rain events in this region. The results from regression analysis suggest that there are no statistically significant correlation between light rain events and favorable water vapor transport (WVT) and convergence pattern. Hence, we found no supporting evidence that the decrease trend in light rain in EC may be related to large-scale changes in moisture conditions. This strongly suggests that other mechanisms may have played a more dominant role in altering the precipitation characteristics in EC during the last 5 decades.

[43] It is known that anthropogenic aerosols from air pollution can affect precipitation via radiative and microphysical effects. Measurements of visual range and pollutant emissions both suggest that aerosol concentrations have dramatically increased from 1960 to 2000 in China due to an unprecedented increase in population and fossil fuel consumption. In EC, the observed PM_{10} concentration, visual range and AOD exhibit a consistent spatial pattern. They are also very well spatially correlated with the pollutant (e.g., sulfur) emissions from human activities, which suggest that anthropogenic emission is the major source of air pollution and atmospheric aerosols in China. Satellite data provide evidence of higher CDNC and smaller droplet size over the polluted regions in EC relative to the surrounding

relatively clean region. The spatial distribution of CDNC is very well correlated with that of PM10, AOD, and visual range, which indicates that higher aerosol concentrations contributed to higher CDNC.

[44] Sensitivity experiments conducted for the studied region on the basis of a cloud-resolving model show that CDNC is increased and cloud droplet size is reduced under heavily polluted conditions, which results in a significant decline in raindrop concentration and a delay in raindrop formation because collision and coalescence are less efficient when cloud drops are small. In addition, much weaker convection under the heavily polluted condition results in much less ice formation and reduces cold rain. Therefore, precipitation frequencies in the low and median rain rates are significantly reduced in the polluted case compared to the clean case. In conclusion, observational evidences and simulations results suggest that the decreased frequency and amount of light rain could be related to the significant increase in aerosol particles due to air pollution in China.

[45] It is interesting to note that the observed precipitation (see section 2) did not show an evident decline in heavier precipitation larger than 10 mm d^{-1}. We argue that light rain is more susceptible to aerosol effects, but median to heavy rain could be influenced more by the large-scale ambient factors such as circulation and moisture (e.g., SEC in this study). As noted by *Rosenfeld et al.* [2008], suppression of precipitation by aerosols from shallow clouds may result in an increase in precipitation from deeper clouds at the cloud scale [*Rosenfeld et al.*, 2008]. This has been demonstrated by some modeling studies that show that delay of early rain by aerosols can result in greater amounts of cloud water and rain intensities at the later stage of the cloud [*Liu et al.*, 2002; *Tao et al.*, 2007; *Philips et al.*, 2007]. This suggests that aerosols may shift precipitation rates from light to moderate and heavy rains, as discussed in section 2.3 (Figure 5).

[46] One complicating factor is how aerosols may influence precipitation through their influence on the atmospheric environments. For example, besides PW and WVT, atmospheric stability and vertical motion could also affect precipitation. Previous studies suggest that changes in the latter (atmospheric stability and vertical motion) could be related to aerosols as they cool the surface (by scattering and absorption of sunlight through the atmosphere) and warms the atmosphere (by absorption of sunlight) [*Ramanathan et al.*, 2005; *Lau et al.*, 2006]. To examine this factor, we calculated long-term changes in atmospheric stability and vertical motion on the basis of the ERA-40 data from 1958 to 2002 (not shown). We found no evident trend for static stability over NEC but a decreasing trend over SEC (-0.14 k $decade^{-1}$). Consistent with the stability trend, there is no evident trend in vertical motion over NEC, but a trend of enhanced ascending motion is found in SEC. Similar to the changes of PW and WVT discussed in section 3, the observed trends of atmospheric stability and vertical motion may be used to explain the increase of total precipitation in SEC. However, they contradict the significant decrease in light rain in EC.

[47] In summary, this study provides strong and further observational evidence that the precipitation characteristics in EC have changed in the past 5 decades. Analyses of air pollution data, satellite data, and large-scale circulation all suggest that aerosols may have played a more dominant role in the observed decrease trend in light rain in EC. Additionally, our cloud resolving modeling results support the hypothesis that high aerosol concentration under heavily polluted condition could reduce precipitation at the lower rates for convection-induced clouds (including stratiform and anvils). Together with the more solid evidence from previous studies that aerosols suppress precipitation in shallow and warm clouds, we suggest that the significantly increased aerosol concentrations should at least be partly responsible for the observed decline in light rain events observed in eastern China in the past 50 years.

[48] **Acknowledgments.** We thank William I. Gustafson Jr. for his internal review and constructive comments. This research is sponsored by the U.S. Department of Energy's Office of Science Biological and Environmental Research under a bilateral agreement with the China Ministry of Science and Technology on regional climate research. PNNL is operated for the U.S. DOE by Battelle Memorial Institute under contract DE-AC06-76RLO1830. This research was also partly supported by projects 2006CB400505 and GYHY200706010. The ECWMF reanalysis data used in this study were obtained from the ECMWF server available at http://data.ecmwf.int.

References

Ackerman, A. S., O. B. Toon, D. E. Stevens, and J. A. Coakley (2003), Enhancement of cloud and suppression of nocturnal drizzle in stratocumulus polluted haze, *Geophys. Res. Lett.*, *30*(7), 1381, doi:10.1029/2002GL016634.

Andreae, M. O. (2004), Smoking rain clouds over the Amazon, *Science*, *303*, 1337, doi:10.1126/science.1092779.

Bell, T. L., D. Rosenfeld, K.-M. Kim, J.-M. Yoo, M.-I. Lee, and M. Hahnenberger (2008), Midweek increase in U. S. summer rain and storm heights suggests air pollution invigorates rainstorms, *J. Geophys. Res.*, *113*, D02209, doi:10.1029/2007JD008623.

Bennartz, R. (2007), Global assessment of marine boundary layer cloud droplet number concentration from satellite, *J. Geophys. Res.*, *112*, D02201, doi:10.1029/2006JD007547.

Bennartz, R., and Harshvardhan (2007), Correction to "Global assessment of marine boundary layer cloud droplet number concentration from satellite", *J. Geophys. Res.*, *112*, D16302, doi:10.1029/2007JD008841.

Bigg, E. K. (1953), The formation of atmospheric ice crystals by the freezing of droplets, *Q. J. R. Meteorol. Soc.*, *79*, 510–519, doi:10.1002/qj.49707934207.

Brenguier, J. L., et al. (2000), Radiative properties of boundary layer clouds: Droplet effective radius versus number concentration, *J. Atmos. Sci.*, *57*, 803–821, doi:10.1175/1520-0469(2000)057<0803:RPOBLC>2.0.CO;2.

Chan, C. K., and X. H. Yao (2008), Air pollution in mega cities in China, *Atmos. Environ.*, *42*, 1–42, doi:10.1016/j.atmosenv.2007.09.003.

Cheng, Y.-J., J.-H. Zhang, Y.-F. Luo, Z.-T. Liu, G. Lesins, and U. Lohmann (2005), Contribution of changes in sea surface temperature and aerosol loading to the decreasing precipitation trend in southern China, *J. Clim.*, *18*, 1381–1390, doi:10.1175/JCLI3341.1.

Choi, Y.-S., C.-H. Ho, D. Chen, Y.-H. Noh, and C.-K. Song (2008), Spectral analysis of weekly variation in PM10 mass concentration and meteorological conditions over China, *Atmos. Environ.*, *42*, 655–666, doi:10.1016/j.atmosenv.2007.09.075.

Ding, Y. H., Y. Zhang, Q. Ma, and G. Q. Hu (2001), Analysis of the large-scale circulation features and synoptic systems in East Asia during the intensive observation period of GAME/HUBEX, *J. Meteorol. Soc. Jpn.*, *79*, 277–300, doi:10.2151/jmsj.79.277.

Endo, N., B. Ailikun, and T. Yasunari (2005), Trends in precipitation amounts and the number of rainy days and heavy rainfall events during summer in china from 1961 to 2000, *J. Meteorol. Soc. Jpn.*, *83*, 621–631, doi:10.2151/jmsj.83.621.

Fan, J., R. Zhang, G. Li, W.-K. Tao, and X. Li (2007a), Simulations of cumulus clouds using a spectral microphysics cloud-resolving model, *J. Geophys. Res.*, *112*, D04201, doi:10.1029/2006JD007688.

Fan, J., R. Zhang, G. Li, and W.-K. Tao (2007b), Effects of aerosols and relative humidity on cumulus clouds, *J. Geophys. Res.*, *112*, D14204, doi:10.1029/2006JD008136.

Fan, J., R. Zhang, W.-K. Tao, and K. I. Mohr (2008), Effects of aerosol optical properties on deep convective clouds and radiative forcing, *J. Geophys. Res.*, *113*, D08209, doi:10.1029/2007JD009257.

Fan, J., M. Ovtchinnikov, J. Comstock, S. McFarlane, and A. Khain (2009), Ice formation in Arctic mixed-phase clouds: Insights from a 3-D cloud-

resolving model with size-resolved aerosol and cloud microphysics, *J. Geophys. Res.*, *114*, D04205, doi:10.1029/2008JD010782.
Fu, J., W. Qian, X. Lin, and D. Chen (2008), Trends of graded precipitation days in China from 1961 to 2000, *Adv. Atmos. Sci.*, *25*(2), 267–278, doi:10.1007/s00376-008-0267-2.
Gao, J., J. Wang, S. H. Cheng, L. K. Xue, H. Z. Yan, L. J. Hou, Y. Q. Jiang, and W. X. Wang (2007), Number concentration and size distributions of submicron particles in Jinan urban area: Characteristics in summer and winter, *J. Environ. Sci.*, *19*, 1466–1473, doi:10.1016/S1001-0742(07)60239-3.
Gao, X., Y. Luo, W. Lin, Z. Zhao, and F. Giorgi (2003), Simulation of effects of land use change on climate in China by a regional climate model, *Adv. Atmos. Sci.*, *20*(4), 583–592, doi:10.1007/BF02915501.
Giorgi, F., X. Q. Bi, and Y. Qian (2002), Direct radiative forcing and regional climate effects of anthropogenic aerosols over East Asia: A regional coupled climate-chemistry/aerosol model study, *J. Geophys. Res.*, *107*(D20), 4439, doi:10.1029/2001JD001066.
Giorgi, F., X. Bi, and Y. Qian (2003), Indirect vs. direct climatic effects of anthropogenic sulfate over East Asia as simulated with a regional coupled climate-chemistry/aerosol model, *Clim. Change*, *58*, 345–376, doi:10.1023/A:1023946010350.
Gong, D. Y., and C.-H. Ho (2002), Shift in the summer rainfall over the Yangtze river valley in the late 1970s, *Geophys. Res. Lett.*, *29*(10), 1436, doi:10.1029/2001GL014523.
Gong, D. Y., and S. W. Wang (2000), Severe summer rainfall in China associated with enhanced global warming, *Clim. Res.*, *16*(1), 51–59.
Gong, D.-Y., P.-J. Shi, and J.-A. Wang (2004), Daily precipitation changes in semiarid region over northern China, *J. Arid Environ.*, *59*, 771–784, doi:10.1016/j.jaridenv.2004.02.006.
Gong, D.-Y., C.-H. Ho, D. Chen, Y. Qian, Y.-S. Choi, and J. Kim (2007), Weekly cycle of aerosol-meteorology interaction over China, *J. Geophys. Res.*, *112*, D22202, doi:10.1029/2007JD008888.
Ho, C.-H., J.-H. Kim, K.-M. Lau, K.-M. Kim, D.-Y. Gong, and Y.-B. Lee (2005), Interdecadal changes in heavy rainfall in China during the northern summer, *Terr. Atmos. Oceanic Sci.*, *16*(5), 1163–1176.
Hu, Z.-Z., S. Yang, and R. Wu (2003), Long-term climate variations in China and global warming signals, *J. Geophys. Res.*, *108*(D19), 4614, doi:10.1029/2003JD003651.
Huang, Y., W. L. Chameides, and R. E. Dickinson (2007), Direct and indirect effects of anthropogenic aerosols on regional precipitation over east Asia, *J. Geophys. Res.*, *112*, D03212, doi:10.1029/2006JD007114.
Kaiser, D. P., and Y. Qian (2002), Decreasing trends in sunshine duration over China for 1954–1998: Indication of increased haze pollution?, *Geophys. Res. Lett.*, *29*(21), 2042, doi:10.1029/2002GL016057.
Khain, A. P., and A. Pokrovsky (2004), Simulation of effects of atmospheric aerosols on deep turbulent convective clouds using a spectral microphysics mixed-phase cumulus cloud model, Part II: Sensitivity study, *J. Atmos. Sci.*, *61*, 2983–3001, doi:10.1175/JAS-3281.1.
Khain, A. P., D. Rosenfeld, and A. Pokrovsky (2005), Aerosol impact on the dynamics and microphysics of deep convective clouds, *Q. J. R. Meteorol. Soc.*, *131*, 2639–2663, doi:10.1256/qj.04.62.
Khain, A., N. BenMoshe, and A. Pokrovsky (2008), Factors determining the impact of aerosols on surface precipitation from clouds: An attempt at classification, *J. Atmos. Sci.*, *65*, 1721–1748, doi:10.1175/2007JAS2515.1.
Khairoutdinov, M. F., and Y. L. Kogan (1999), A large eddy simulation model with explicit microphysics: Validation against aircraft observations of a stratocumulus-topped boundary layer, *J. Atmos. Sci.*, *56*, 2115–2131, doi:10.1175/1520-0469(1999)056<2115:ALESMW>2.0.CO;2.
Khairoutdinov, M. F., and D. A. Randall (2003), Cloud resolving modeling of the ARM summer 1997 IOP: Model formulation, results, uncertainties, and sensitivities, *J. Atmos. Sci.*, *60*, 607–625, doi:10.1175/1520-0469(2003)060<0607:CRMOTA>2.0.CO;2.
Kiehl, J. T., J. J. Hack, G. B. Bonan, B. A. Boville, D. L. Williamson, and P. J. Rasch (1998), The National Center for Atmospheric Research Community Climate Model: CCM3, *J. Clim.*, *11*, 1131–1149, doi:10.1175/1520-0442(1998)011<1131:TNCFAR>2.0.CO;2.
King, M. D., et al. (2003), Cloud and aerosol properties, precipitable water, and profiles of temperature and water vapor from MODIS, *IEEE Trans. Geosci. Remote Sens.*, *41*, 442–458, doi:10.1109/TGRS.2002.808226.
Koren, I. (2005), Aerosol invigoration and restructuring of Atlantic convective clouds, *Geophys. Res. Lett.*, *32*, L14828, doi:10.1029/2005GL023187.
Koren, I., J. V. Martins, L. A. Remer, and H. Afargan (2008), Smoke invigoration versus inhibition of clouds over the Amazon, *Science*, *321*, 946–949, doi:10.1126/science.1159185.
Lau, K.-M., M.-K. Kim, and K.-M. Kim (2006), Asian summer monsoon anomalies induced by aerosol direct forcing: The role of the Tibetan Plateau, *Clim. Dyn.*, *26*(7–8), 855–864, doi:10.1007/s00382-006-0114-z.
Leung, L. R., S. Zhong, Y. Qian, and Y. Liu (2004), Evaluation of regional climate simulations of the 1998 and 1999 East Asian summer monsoon using the GAME/HUBEX observational data, *J. Meteorol. Soc. Jpn.*, *82*, 1695–1713, doi:10.2151/jmsj.82.1695.
Levin, Z., and W. Cotton (2007), *Aerosol Pollution Impact on Precipitation: A Scientific Review. Report From the WMO/IUGG International Aerosol Precipitation Science Assessment Group (IAPSAG)*, World Meteorol. Organ, Geneva, Switzerland.
Levy, R. C., L. Remer, S. Mattoo, E. Vermote, and Y. J. Kaufman (2007), Second-generation algorithm for retrieving aerosol properties over land from MODIS spectral reflectance, *J. Geophys. Res.*, *112*, D13211, doi:10.1029/2006JD007811.
Li, Z., et al. (2007), Preface to special section on East Asian Studies of Tropospheric Aerosols: An International Regional Experiment (EAST-AIRE), *J. Geophys. Res.*, *112*, D22S00, doi:10.1029/2007JD008853.
Lin, J. C., T. Matsui, R. A. Pielke Sr., and C. Kummerow (2006), Effects of biomass-burning-derived aerosols on precipitation and clouds in the Amazon Basin: A satellite-based empirical study, *J. Geophys. Res.*, *111*, D19204, doi:10.1029/2005JD006884.
Liu, B., M. Xu, M. Henderson, and Y. Qi (2005), Observed trends of precipitation amount, frequency, and intensity in China, 1960–2000, *J. Geophys. Res.*, *110*, D08103, doi:10.1029/2004JD004864.
Liu, S. C., C. Wang, C. Shiu, H. Chang, C. Hsiao, and S. Liaw (2002), Reduction in sunshine duration over Taiwan: Causes and implications, *Terr. Atmos. Oceanic Sci.*, *13*(4), 523–545.
Lynn, B., A. Khain, J. Dudhia, D. Rosenfeld, A. Pokrovsky, and A. Seifert (2005), Spectral (bin) microphysics coupled with a mesoscale model (MM5). Part 1: Model description and first results, *Mon. Weather Rev.*, *133*, 44–58, doi:10.1175/MWR-2840.1.
Menon, S., J. Hansen, L. Nazarenko, and Y. F. Luo (2002), Climate effects of black carbon aerosols in China and India, *Science*, *297*, 2250–2253, doi:10.1126/science.1075159.
Meyers, M. P., P. J. DeMott, and W. R. Cotton (1992), New primary ice-nucleation parameterizations in an explicit cloud model, *J. Appl. Meteorol.*, *31*, 708–721, doi:10.1175/1520-0450(1992)031<0708:NPINPI>2.0.CO;2.
Philips, V. T. J., L. J. Donner, and S. T. Garner (2007), Nucleation processes in deep convection simulated by a cloud-system-resolving model with double-moment bulk microphysics, *J. Atmos. Sci.*, *64*, 738–761, doi:10.1175/JAS3869.1.
Platnick, S., et al. (2003), The MODIS cloud products: Algorithms and examples from Terra, *IEEE Trans. Geosci. Remote Sens.*, *41*, 459–473, doi:10.1109/TGRS.2002.808301.
Qian, W., J. Fu, and Z. Yan (2007b), Decrease of light rain events in summer associated with a warming environment in China during 1961–2005, *Geophys. Res. Lett.*, *34*, L11705, doi:10.1029/2007GL029631.
Qian, Y., and F. Giorgi (1999), Interactive coupling of regional climate and sulfate aerosol models over East Asia, *J. Geophys. Res.*, *104*, 6477–6499, doi:10.1029/98JD02347.
Qian, Y., and F. Giorgi (2000), Regional climatic effects of anthropogenic aerosols? The case of southwestern China, *Geophys. Res. Lett.*, *27*, 3521–3524, doi:10.1029/2000GL011942.
Qian, Y., and L. R. Leung (2007), Long-term regional model simulation and observations of the hydroclimate in China, *J. Geophys. Res.*, *112*, D14104, doi:10.1029/2006JD008134.
Qian, Y., C. B. Fu, R. M. Hu, and Z. F. Wang (1996), Effects of industrial SO_2 emission on temperature variation in China and East Asia (in Chinese), *Clim. Environ. Res.*, *2*, 143–149.
Qian, Y., F. Giorgi, Y. Huang, W. L. Chameides, and C. Luo (2001), Regional simulation of anthropogenic sulfur over East Asia and its sensitivity to model parameters, *Tellus, Ser. B*, *53*, 171–191.
Qian, Y., L. R. Leung, S. J. Ghan, and F. Giorgi (2003), Regional climate effects of aerosols over China: Modeling and observation, *Tellus, Ser. B*, *55*, 914–934.
Qian, Y., D. P. Kaiser, L. R. Leung, and M. Xu (2006), More frequent cloud-free sky and less surface solar radiation in China from 1955 to 2000, *Geophys. Res. Lett.*, *33*, L01812, doi:10.1029/2005GL024586.
Qian, Y., W. Wang, L. R. Leung, and D. P. Kaiser (2007a), Variability of solar radiation under cloud-free skies in China: The role of aerosols, *Geophys. Res. Lett.*, *34*, L12804, doi:10.1029/2006GL028800.
Radke, L. F. (1989), Direct and remote-sensing observations of the effects of ships on clouds, *Science*, *246*, 1146–1149, doi:10.1126/science.246.4934.1146.
Ramanathan, V., P. J. Crutzen, J. T. Kiehl, and D. Rosenfeld (2001), Aerosols, climate, and the hydrological cycle, *Science*, *294*, 2119–2124, doi:10.1126/science.1064034.
Ramanathan, V., C. Chung, D. Kim, T. Bettge, L. Buja, J. T. Kiehl, W. M. Washington, Q. Fu, D. R. Sikka, and M. Wild (2005), Atmospheric brown clouds: Impact on South Asian climate and hydrologic cycle, *Proc. Natl. Acad. Sci. U. S. A.*, *102*, 5326–5333, doi:10.1073/pnas.0500656102.

Ramaswamy, V. (2001), Radiative forcing of climate change, in *Climate Change 2001: The Scientific Basis: Contribution of Working Group I to the Third Assessment Report of the Intergovernmental Panel on Climate Change*, edited by J. T. Houghton et al., pp. 349–416, Cambridge Univ. Press, Cambridge, U. K.

Remer, L. A. (2008), Global aerosol climatology from the MODIS satellite sensors, *J. Geophys. Res.*, *113*, D14S07, doi:10.1029/2007JD009661.

Ren, Z. H., Z. Y. Jiang, X. X. Yang, and Q. X. Gao (1997), Research on the atmospheric transportaion, deposition and mutual influence of interprovince of acid materials over China, in *Acid Rain and its Control Issue in China (in Chinese)*, *World Lab. Workshop Ser.*, vol. 78, pp. 75–96, China Cent. of Adv. Sci. and Technol., Beijing.

Ren, G. Y., H. Wu, and Z. H. Chen (2000), Spatial patterns of change trend in rainfall of China (in Chinese), *Q. J. Appl. Meteorol.*, *11*(3), 322–330.

Riches, M. R., W. C. Wang, P. Chen, S. Tao, S. Zhou, and Y. Ding (2000), Recent progress in the joint agreements on "Global and Regional Climate Change" studies between the United States and the People's Republic of China, *Bull. Am. Meteorol. Soc.*, *81*(3), 491–500, doi:10.1175/1520-0477(2000)081<0491:RPITJA>2.3.CO;2.

Rosenfeld, D. (1999), TRMM observed first direct evidence of smoke from forest fires inhibiting rainfall, *Geophys. Res. Lett.*, *26*, 3105–3108, doi:10.1029/1999GL006066.

Rosenfeld, D. (2000), Suppression of rain and snow by urban and industrial air pollution, *Science*, *287*, 1793–1796, doi:10.1126/science.287.5459.1793.

Rosenfeld, D. (2006), Aerosols, clouds, and climate, *Science*, *312*, 1323–1324, doi:10.1126/science.1128972.

Rosenfeld, D., Y. Rudich, and R. Lahav (2001), Desert dust suppressing precipitation: A possible desertification feedback loop, *Proc. Natl. Acad. Sci. U. S. A.*, *98*, 5975–5980, doi:10.1073/pnas.101122798.

Rosenfeld, D., J. Dai, X. Yu, Z. Y. Yao, X. H. Xu, X. Yang, and C. L. Du (2007), Inverse relations between amounts of air pollution and orographic precipitation, *Science*, *315*, 1396–1398, doi:10.1126/science.1137949.

Rosenfeld, D., U. Lohmann, G. B. Raga, C. D. O'Dowd, M. Kulmala, S. Fuzzi, A. Reissell, and M. O. Andreae (2008), Flood or drought: How do aerosols affect precipitation?, *Science*, *321*, 1309–1313, doi:10.1126/science.1160606.

Shi, Z. B., K. B. He, X. C. Yu, Z. L. Yao, F. M. Yang, Y. L. Ma, R. Ma, Y. T. Jia, and J. Zhang (2007), Diurnal variation of number concentration and size distribution of ultrafine particles in the urban atmosphere of Beijing in winter, *J. Environ. Sci.*, *19*, 933–938, doi:10.1016/S1001-0742(07)60154-5.

Simmonds, I., D. Bi, and P. Hope (1999), Atmospheric water vapor flux and its association with rainfall over China in summer, *J. Clim.*, *12*, 1353–1367, doi:10.1175/1520-0442(1999)012<1353:AWVFAI>2.0.CO;2.

Tang, X. Y. (2004), The characteristics of urban air pollution in China, in *Urbanization, Energy, and Air Pollution in China: The Challenges Ahead*, pp. 47–54, Chinese Acad. of Eng., Beijing, China.

Tao, W.-K., X. Li, A. Khain, T. Matsui, S. Lang, and J. Simpson (2007), Role of atmospheric aerosol concentration on deep convective precipitation: Cloud-resolving model simulations, *J. Geophys. Res.*, *112*, D24S18, doi:10.1029/2007JD008728.

Uppala, S. M., et al. (2005), The ERA-40 re-analysis, *Q. J. R. Meteorol. Soc.*, *131*, 2961–3012, doi:10.1256/qj.04.176.

Wang, J. X. L., and D. J. Gaffen (2001), Late twentieth century climatology and trends of surface humidity and temperature in China, *J. Clim.*, *14*, 2833–2845, doi:10.1175/1520-0442(2001)014<2833:LTCCAT>2.0.CO;2.

Wang, S., and D. Gong (2000), Enhancement of the warming trend in China, *Geophys. Res. Lett.*, *27*, 2581–2584, doi:10.1029/1999GL010825.

Wilks, D. S. (1995), *Statistical Methods in the Atmospheric Sciences: An Introduction*, 467 pp., Academic, San Diego, Calif.

Williams, E., et al. (2002), Contrasting convective regimes over the Amazon: Implications for cloud electrification, *J. Geophys. Res.*, *107*(D20), 8082, doi:10.1029/2001JD000380.

Xu, Q. (2001), Abrupt change of the mid-summer climate in central east China by the influence of atmospheric pollution, *Atmos. Environ.*, *35*, 5029–5040, doi:10.1016/S1352-2310(01)00315-6.

Zhai, P., and R. E. Eskridge (1997), Atmospheric water vapor over China, *J. Clim.*, *10*, 2643–2652, doi:10.1175/1520-0442(1997)010<2643:AWVOC>2.0.CO;2.

Zhai, P.-M., A.-J. Sun, F.-M. Ren, X.-N. Liu, B. Gao, and Q. Zhang (1999), Changes of climate extremes in China, *Clim. Change*, *42*, 203–218, doi:10.1023/A:1005428602279.

Zhai, P.-M., X.-B. Zhang, H. Wan, and X.-H. Pan (2005), Trends in total precipitation and frequency of daily precipitation extremes over China, *J. Clim.*, *18*, 1096–1108, doi:10.1175/JCLI-3318.1.

Zhao, C., X. Tie, and Y. Lin (2006), A possible positive feedback of reduction of precipitation and increase in aerosols over eastern central China, *Geophys. Res. Lett.*, *33*, L11814, doi:10.1029/2006GL025959.

Zhou, T.-J., and R.-C. Yu (2005), Atmospheric water vapor transport associated with typical anomalous summer rainfall patterns in China, *J. Geophys. Res.*, *110*, D08104, doi:10.1029/2004JD005413.

R. Bennartz, Department of Atmospheric and Oceanic Sciences, University of Wisconsin, Madison, WI 53706, USA.

D. Chen, Department of Earth Sciences, University of Gothenburg, SE-405 30 Gothenburg, Sweden.

J. Fan, L. R. Leung, Y. Qian, and W. Wang, Atmospheric Science and Global Change Division, Pacific Northwest National Laboratory, 902 Battelle Boulevard, Richland, WA 99352, USA. (yun.qian@pnl.gov)

D. Gong, State Key Laboratory of Earth Surface Processes and Resource Ecology, Beijing Normal University, Beijing 100875, China.